Optimal Design of the Composite Laminate Vessel Based on SCGM

David T.W. Lin[1,*], *Pham Duy Hai*[1], *Chin-Hsiang Cheng*[2]

[1] *Institute of Mechatronic System Engineering, National University of Tainan, Taiwan*

[2] *Department of Aeronautics and Astronautics, National Cheng Kung University*

***Abstract* - The purpose of this study is to optimize the design of the composite laminate vessel for minimizing the stress concentration. The optimum design of this study uses the finite element method combined with the simplified conjugated gradient method (SCGM) to find the minimization of Von Mises stress of the vessel. In this study, the composite laminate vessel with the aluminum liner and the carbon fiber/epoxy layer are considered. The winding angle and the thickness of composite layer are proposed as the optimal design variables. Through this optimization, the best combination of the thickness and the winding angle of composite layer can be obtained to reach the minimum stress concentration.**

***Index Terms*--Composite laminate vessel, Stress concentration, Optimal design, SCGM**

I. Introduction

The composite laminate vessel consists of a thin, non-structural liner wrapped with a structural fiber composite, designed to hold hydrogen fuel under the designed pressure. The most material commonly used to wrap the composite pressure vessel is fiber reinforced polymers (FRP), carbon or Kevlar fibers. Carbon fiber is most popular used as a composite laminated structure.

In recent years, many previous studies related the composite laminates have been examined, such as the stress and optimal design [1, 2], the combining of internal pressure and thermo mechanical loading [3, 4], the analytical analysis [5] and progressive failure analysis [6]. The failure analysis of the fiber/aluminum liner composite laminates is studied in the application of the hydrogen storage vessel [7, 8]. Liu and Tsai [9] build the progressive quadratic failure criterion in the failure analysis for laminated composites.

A large amount of research is presented many methods to optimize the composite laminate with various purposes such as minimum weight, strength and stiffness, such as the simple mathematic method [10-14], deterministic and stochastic algorithm [15], artificial immune system [16] and the gradient search method [17].

This research is to demonstrate how the application of numerical optimal simulation techniques can be used to search for an effective and robust optimization of the vessel design. Therefore, the optimal design of the pressure vessel for obtaining the minimum stress concentration is achieved in the present study. The numerical design is developed by combining a direct finite element solver with an optimal method (the simplified conjugate gradient method, SCGM [18]). A finite element analysis model ANSYS is used as the subroutine to solve the stress-strain profile associated with the variation of the geometry of the vessel during the iterative optimal process.

II. Numerical analysis and optimization methods

The following analysis focuses on the cylindrical part of composite vessel. The cylindrical part of composite vessel consists of two parts. The first part is made of 6061-T6 aluminum liner layer and the second part is n_s carbon fiber/epoxy composite layers. The liner is considered to be an isotropic and the carbon fiber/epoxy composite is transversely isotropic. The winding angles at the cylinder is 90°, -90°, α_0, -α_0, …, α_0, -α_0, 90°, -90° in turn.

The outer radii of the cylindrical structures is written as

$$r_o = r_i + e_1 + n_s e_c \quad (1)$$

where e_1, e_c is the thicknesses of the liner and single composite winding layer, r_i is the inner radii of the cylindrical structures.

For the k^{th} layer, the equilibrium equation in the absence of body forces under the cylindrical coordinate is given by

$$\frac{1}{r}\frac{\partial(r\sigma_r^{(k)})}{\partial r} - \frac{\sigma_\theta^{(k)}}{r} = 0 \quad (2)$$

The stress-strain relationships of the k^{th} layer for anisotropic materials are expressed by

$$\begin{bmatrix} \sigma_z \\ \sigma_\theta \\ \sigma_r \\ \tau_{z\theta} \end{bmatrix}^k = \begin{bmatrix} \bar{C}_{11} & \bar{C}_{12} & \bar{C}_{13} & \bar{C}_{16} \\ \bar{C}_{21} & \bar{C}_{22} & \bar{C}_{23} & \bar{C}_{26} \\ \bar{C}_{13} & \bar{C}_{23} & \bar{C}_{33} & \bar{C}_{36} \\ \bar{C}_{26} & \bar{C}_{26} & \bar{C}_{36} & \bar{C}_{66} \end{bmatrix}^k \begin{bmatrix} \varepsilon_z \\ \varepsilon_\theta \\ \varepsilon_r \\ \gamma_{z\theta} \end{bmatrix}^k \quad (3)$$

where $\bar{C}_{ij}(i, j = 1,2,3,6)$ is the off-axis elastic constants of materials.

In terms of small deformation, the strain-displacement relationships are written as

$$\varepsilon_z^{(k)} = \frac{du_z^{(k)}}{dz} = \varepsilon_0,\ \gamma_{z\theta}^{(k)} = \frac{du_\theta^{(k)}}{dz} = \gamma_0 r \quad (4)$$

where γ_0 is twist per unit length.

The radial displacement of the k^{th} layer is calculated as [19]

$$u_r^{(k)} = A^{(k)} r^{\beta(k)} + B^{(k)} r^{-\beta(k)} + \lambda_1^{(k)} r + \gamma_0 r^2 \quad (5)$$

* Corresponding author: david@mail.nutn.edu.tw

where

$$\beta(k)=\sqrt{\frac{\bar{C}_{22}^{(k)}}{\bar{C}_{33}^{(k)}}} \tag{6}$$

$$\lambda_1^{(k)}=\lambda_3^{(k)}\varepsilon_0+\lambda_4^{(k)}\Delta T=\frac{(\bar{C}_{12}^{(k)}-\bar{C}_{13}^{(k)})\varepsilon_0}{\bar{C}_{33}^{(k)}-\bar{C}_{22}^{(k)}}+\frac{(\eta_3^{(k)}-\eta_2^{(k)})}{\bar{C}_{33}^{(k)}-\bar{C}_{22}^{(k)}} \tag{7}$$

$$\lambda_2^{(k)}=\frac{\bar{C}_{26}^{(k)}-2\bar{C}_{36}^{(k)}}{4\bar{C}_{33}^{(k)}-\bar{C}_{22}^{(k)}} \tag{8}$$

For anisotropic materials, $\bar{C}_{22}^{(k)}/\bar{C}_{33}^{(k)}>0$ and $\bar{C}_{22}^{(k)}/\bar{C}_{33}^{(k)}\neq 0$ are approved. From the Eqs. (1)-(5), the radial, hoop and shear-stress of each layer can be obtained, respectively [1].

If the carbon fiber/epoxy composite layers are considered transversely isotropic with same elastic properties on the plane (2-3), the on-axis stiffness matrix $C^{(k)}$ of the k^{th} layer is given by

$$C^{(k)}=[S^{(k)}]^{-1} \tag{9}$$

$$S^{(k)}=\begin{bmatrix} \frac{1}{E_1} & -\frac{v_{12}}{E_1} & -\frac{v_{12}}{E_1} & 0 & 0 & 0 \\ -\frac{v_{12}}{E_1} & \frac{1}{E_2} & -\frac{v_{23}}{E_1} & 0 & 0 & 0 \\ -\frac{v_{12}}{E_1} & -\frac{v_{23}}{E_1} & \frac{1}{E_2} & 0 & 0 & 0 \\ 0 & 0 & 0 & \frac{2(1+v_{23})}{E_2} & 0 & 0 \\ 0 & 0 & 0 & 0 & \frac{2(1+v_{12})}{E_2} & 0 \\ 0 & 0 & 0 & 0 & 0 & \frac{2(1+v_{12})}{E_2} \end{bmatrix} \tag{10}$$

where S and C is the on-axis compliance and stiffness tensors, v is the Poisson's ratio, respectively.

By introducing a stiffness transformation matrix $T_s(\phi)$ which is a function of the angle ϕ, the relationships between the off-axis and on-axis elastic constants are expressed as

$$\bar{C}=T_s(\phi)CT_s^T(\phi) \tag{11}$$

$$T_c(\phi)=\begin{bmatrix} m^2 & n^2 & 0 & 0 & 0 & mn \\ n^2 & m^2 & 0 & 0 & 0 & -mn \\ 0 & 0 & 1 & 0 & 0 & 0 \\ 0 & 0 & 0 & m & -n & 0 \\ 0 & 0 & 0 & n & m & 0 \\ -2mn & 2mn & 0 & 0 & 0 & m^2-n^2 \end{bmatrix} \tag{12}$$

$$T_s(\phi)=[(T_e(\phi))^{-1}]^T \tag{13}$$

where m, n is $\cos\phi$ and $\sin\phi$, respectively.

Thus, the off-axis stress is obtained by

$$\bar{\sigma}=T_s\sigma \tag{14}$$

where $\bar{\sigma}$ and σ is the off-axis and on-axis stress tensors, respectively.

Failure criteria

The maximum shear stress and Tsai-Wu failure criteria are considered for the liner material and carbon fiber/epoxy composite layers, respectively. The quadratic Tsai-Wu failure surface for a 3D stress state is expressed in the following form

$$F(\sigma)=F_i\sigma_i+F_{ij}\sigma_i\sigma_j=1, \qquad i,j=1,2,...6 \tag{15}$$

where F_i and F_{ij} is the second-order and fourth-order strength tensors depending on the tensile, compressive and shear strengths of the composites, respectively.

For the anisotropic composite laminate, the quadratic Tsai-Wu failure criterion can be written in the following form

$$F_{11}\sigma_1^2+F_{22}\sigma_2^2+F_{66}\sigma_6^2+F_1\sigma_1+F_2\sigma_2+2F_{12}\sigma_1\sigma_2\geq 1 \tag{16}$$

where σ_1 and σ_2 is the on-axis stresses in the longitudinal and transverse directions, and σ_6 is the on-axis in-plane shear stress.

The strength parameters F_{11}, F_{22}, F_{66}, F_1, F_2 and F_{12} are given by

$$F_{11}=\frac{1}{X_tX_c},\quad F_{22}=\frac{1}{Y_tY_c},\quad F_{66}=\frac{1}{S^2}$$
$$F_1=\frac{1}{X_t}-\frac{1}{X_c},\quad F_2=\frac{1}{Y_t}-\frac{1}{Y_c} \tag{17}$$
$$F_{12}=-\frac{1}{2}\sqrt{F_{11}F_{22}}$$

where

X_t and X_c: the longitudinal tensile and compressive strengths, respectively.

Y_t and Y_c: the transverse tensile and compressive strengths, respectively.

S: the in-plane shear strength.

Modeling description

The 6061 Al-T6 liner-carbon and 700 fiber/0164 epoxy composites are employed for numerical calculations. The number of the number of the composite layer is n_s = 10. The thickness of each composite layer is 1.2 mm and the liner is 3 mm. The capacity of the composite vessel is V = 0.01 m^3, the inner radius and length of cylinder are 100 mm and 220 mm, respectively. At the head of model, *NE*, *RI* and *RO* have dimensions 50 mm, 7 mm and 11 mm, respectively. The working pressure is assumed as 40 MPa. A 30° axisymmetric parametric finite element model is established, the 3D eight-node solid element SOLID95 and 3D eight-node anisotropic solid element SOLID64 are adopted from ANSYS.

Fig. 1 shows the mesh model with mesh element of composite pressure vessel for analysis which assembled from a 6061-T6 aluminum liner layer and 10 layers of carbon fiber/epoxy composite is presented for analysis.

Optimization method

The objective function J of this study is the minimum Von Mises stress of the vessel. The Von Mises stress (as known as equivalent stress σ_{eqv}) is given by:

$$J = \sigma_{eqv} = \sqrt{\frac{(\sigma_i - \sigma_t)^2 + (\sigma_t - \sigma_r)^2 + (\sigma_r - \sigma_i)^2}{2}} \quad (18)$$

where σ_i, σ_t and σ_r is the longitudinal, tangential and radial stresses, respectively.

The SCGM method is capable of obtaining the minimized objective functions easily, and calculating fast than traditional conjugated gradient method. This method is successfully employed in the optimization of the heat concentration on the high power LED array [18], the design of the flexible pyroelectric temperature sensor [20] and the LED package [21].

Beside, IA is the iteration number in the optimal design process.

In addition, we assume $\{a_i,\ i = 1,2,...,l\}$ be the set of the undetermined coefficients. The variables a_i are treated as the optimal variables which are to be designed in this study to minimize the objective function. Different combinations of these coefficients represent the variation of the pressure vessel's geometry. In other words, in the optimization process, the undetermined coefficients are updated iteratively toward the minimization of the object function.

In this manner, as the objective function is approaching its minimum value in the optimal process, with the definition of J, the temperature distribution gradually reaches a uniform distribution. This implies that the phenomena of stress concentration will be decreased.

The minimization of the objective function is accomplished by using the SCGM. The method evaluates the gradient functions of the objective function and sets up a new conjugate direction for the updated undetermined coefficients with the help of a direct numerical sensitivity analysis.

We perform the direct numerical sensitivity analysis to determine the gradient functions $\left\{\left(\partial J/\partial a_i\right)^n,\ i = 1,2,...,l\right\}$ in the n_{th} step. First, give a perturbation (Δa_i) to each of the undetermined coefficients, and then find the change of the objective function (ΔJ) caused by Δa_i. The gradient function with respect to each of the undetermined coefficients can be calculated by the direct numerical differentiation as

$$\frac{\partial J}{\partial a_i} = \frac{\Delta J}{\Delta a_i} \quad (19)$$

Then, we can calculate the conjugate gradient coefficients, γ_i^n, and the search directions, π_i^{n+1}, for each of the undetermined coefficients with

$$\gamma_i^n = \left[\frac{\left(\frac{\partial J}{\partial a_i}\right)^n}{\left(\frac{\partial J}{\partial a_i}\right)^{n-1}}\right]^2,\quad i = 1,2,\ldots,l \quad (20)$$

$$\pi_i^{n+1} = \left(\frac{\partial J}{\partial a_i}\right)^n + \gamma_i^n \pi_i^n,\quad i = 1,2,\ldots,l \quad (21)$$

The step sizes $\{\tau_i,\ i = 1,2,...,l\}$ will be assigned for all the undetermined coefficients and leave it unchanged during the iteration. In this study, the fixed value is determined by a trial and error process, and the value is set to be 1.0×10^{-6} typically. The difficulty lies with the fact that how to decide the suitable value of the step size. The undetermined coefficients will be updated.

$$a_i^{n+1} = a_i^n - \tau_i \pi_i^{n+1},\quad i = 1,2,...,l \quad (22)$$

The procedure for applying the SCGM method is described briefly in the following:

(1) Make an initial guess for the shape profile by giving initial values to the set of undetermined coefficients. With initialization accomplished, the run itself can begin.
(2) Use the direct problem solver to predict the stress concentration and stress distribution of the pressure vessel, and calculate the objective function J by Eq. (18).
(3) When the objective function reaches a minimum, that is to say, the relative criteria is satisfied, the solution process is terminated. Otherwise, proceed to step (4).
(4)Through the Eq. (19), to determine the gradient functions.
(5) Through the Eqs. (20) and (21), to calculate the conjugate gradient coefficients, γ_i^n, and the search directions, π_i^{n+1}, for each of the undetermined coefficients.
(6) Assign a fixed value to the step sizes for all the undetermined coefficients and leave it unchanged during the iteration.
(7) According the Eq. (22), to update the undetermined coefficients and re-new the geometry of the pressure vessel, and go back to step (2).

It is important to mention that the emphasis of present study is put on the optimization of the pressure vessel. To the authors' knowledge, it's a new view to deal the stress-strain problem by using the optimal method of SCGM.

Figure 2 presents a flow chart of the optimization process. Note that the optimizer (SCGM) is integrated with the ANSYS code by means of a self-developed interface program written in APDL script. As shown in Fig. 2, the values of the undetermined coefficients suggested by the optimizer are sent to the direct problem solver in order to update the geometrical model and grid system. The direct problem solver then utilizes this updated information to determine the stress of the pressure vessel and to compute the corresponding value of the objective function. The outputs of the direct problem solver are then transferred back to the optimizer in order to calculate the new iteration.

III. RESULTS AND DISCUSSIONS

This research aims to design the optimal composite laminate vessel. The objective function of this design is to approach the minimum stress concentration under the internal pressure P=40 MPa. The simplified conjugate gradient method (SCGM) is used as the optimal algorithm. This study discusses the variables of composite layer (h) and the winding angle (α_0). The range of the thickness of composite layer is bounded from 1.2 mm to 1.6 mm and the bounded of the winding angle from 10° to 45° for the condition of optimal process.

The stress distribution of initial model is shown in Fig. 3. Here, a 30° axisymmetric finite element model is used. The simulated region is from the center of the cylinder part to the head. The winding angles of each composite layers from the inner 1^{st} layer to the outer layers are 90°, -90°, 18.9°, -18.9°, 90°, -90°, 18.9°, -18.9°, 90°, -90°, respectively and the thickness is 1.2 cm. A cylindrical coordinate system is defined and r, θ, z denote the radial, hoop and axial directions, respectively. Perfect bonding between the aluminum liner layer and carbon fiber/epoxy composite layers are assumed. The symmetric constraints are acting on the symmetric sides and the pressure P is loaded on the inner surface of the liner layer. The result of this initial model exists a high stress concentration (687.83 MPa) appeared on outer composite layers of model. The location is close to the bottom of the simulated region, i.e. the center of the cylinder part.

Using SCGM in the optimal process shows the profile of the stress concentration in Fig. 4. Here, the step size of SCGM is 0.01 which is the best step size evaluated among the three values including 0.01, 0.001 and 0.005. The stress concentration drops dramatically up to approximately 490 MPa then decreases slightly approaching the optimal stress concentration is 490.03 MPa with the iteration is 138 and the winding angle is 36.2° and 1.6mm thickness. The optimal thickness of the pressure vessel is the maximum thickness in the variable range. It matches the well-received knowledge. We still assume two variables to process the optimal calculation, but emphasis the effect of the winding angle not the well-received results of the thickness of pressure vessel.

The effect of the winding angle will be discussed in details for enhancing the knowledge of the composite pressure vessel. Fig. 5 demonstrates the profile of stress concentration with the winding angle from 10° to 45° at the thickness of composite layer is 1.6 mm. The stress concentration increases from 497.62 MPa to 498.28 MPa as the winding angle is changed from 10° to 13° and decreases from 498.28 MPa to 489.54 MPa from 13° to 36.54°, then rises up from the minimum value to 496.56 MPa as the winding angle increases to 45°. The reduced stress resulted from the variation of winding angle is 8.74 MPa, about 6% of the effect of the layer thickness. This study depends on the optimal method to search the optimal winding angle and obtain the result.

IV. CONCLUSIONS

This paper presents the optimal method (SCGM) to obtain the minimum stress concentration of composite pressure vessel. The winding angle and the thickness of the composite layer are the design variables in the optimal process. The optimal result is 489.54 MPa at the thickness of composite layer is 1.6 mm and the winding angle is 36.54^o.

We notice that the variations of all variables will make the benefit of the safety of the pressure vessel. The thickness variable is dominant and the winding angel is still not negligible in this optimal design.

In conclusion, the stress concentration occurred on the region of cylinder part will be reduced through this proposed optimal process. It can be proof that this proposed method is effective. Therefore, the findings and implications of the study should be generalized to the extent that future performance designs of the commercial product development.

V. REFERENCES

[1] C.U. Kim, J.H. Kang, C.S. Hong and C.G. Kim, Optimal design of filament wound type 3 tanks under internal pressure using a modified genetic algorithm, Compos. Struct. 71, pp. 16–25, 2005.

[2] C.U. Kim, J.H. Kang, C.S. Hong and C.G. Kim, Optimal design of filament wound structures under internal pressure based on the semi-geodesic path algorithm, Compos. Struct. 67, pp. 443–452, 2005.

[3] M. Xia, M. Takayanagi and K. Kemmochi, Analysis of multi-layered filament-wound composite pipes under internal pressure, Compos. Struct. 53, pp. 483–491, 2001.

[4] M. Xia, K. Kemmochi and H. Takayanagi, Analysis of filament-wound fiber-reinforced sandwich pipe under combined internal pressure and thermo mechanical loading, Compos. Struct. 51, pp. 273–283, 2001.

[5] L. Parnas and N. Katirci, Design of fiber-reinforced composite pressure vessels under various loading conditions, Compos. Struct. 58, pp. 83–95, 2002.

[6] Travis A. Bogetti, Christopher P. R. Hoppel, Vasyl M. Harik, James F. Newill, Bruce P, Burns Predicting the nonlinear response and progressive failure of composite laminates, Compos. Sci and Tech. 64, pp. 329-342, 2004.

[7] P. Xu, J. Zheng, H. Chen, P. Liu, Optimal design of high pressure hydrogen storage vessel using an adaptive genetic algorithm, Int. J. Hydrogen Energy. pp 1-7, 2009.38

[8] S. Basu, A.M. Waas et al., Prediction of progressive failure in multidirectional composite laminated panels, Int J Solid Struct. 44, pp. 2648–2676, 2007.

[9] K.S. Liu, S.W. Tsai, A progressive quadratic failure criterion for a laminate, Compos Sci and Tech. 58, pp. 1023–1032, 1998.

[10] A.A Smerdov, A computational study in optimum formulations of optimization problems on laminated cylindrical shells for buckling I. Shells under axial compression, Compos. Sci and Tech, 60, pp 2057-2066, 2000.

[11] A.A. Smerdov, A computational study in optimum

formulations of optimization problems on laminated cylindrical shells for buckling II. Shells under external pressure, Compos. Sci and Tech. 60, pp 2067-2076, 2000.

[12] Petri Kere, Juhani Koski, Multicriterion stacking sequence optimization scheme for composite laminates subjected to multiple loading conditions, Compos. Struc. 54, pp 225-229, 2001.

[13] Petri Kere, Mikko Lyly, Juhani Koski, Using multicriterion optimization for strength design of composite laminates, Compos. Struc. 62, pp 329-333, 2003.33

[14] S. Adali, F. Lene, G. Duvaut, V. Chiaruttini, Optimization of laminated composites subject to uncertain buckling load, Compos. Struc. 62, pp 261-269, 2003.

[15] Petr P. Procházka, Deterministic and stochastic optimization of composite cylindrical laminates, Int. J Solids and Struc. 40, 25, pp 7109-7127, 2003.35

[16] Pengfei Liu, Ping Xu, Jinyang Zheng, Artificial immune system for optimal design of composite hydrogen storage vessel, Comput. Mat. Sci. 47, pp. 261-267, 2009.

[17] Bruyneel M, Fleury C, Composite structures optimization using sequential convex programming, Adv. Eng. Software, 33, pp. 697-711, 2002.

[18] J.C. Hsieh, David T.W. Lin, and C.H. Cheng, 2011, "Optimization of thermal management by integration of an SCGM, a finite element method and an experiment on a high power LED array," *IEEE Transaction on Electron Devices*, Vol. 58, No. 4, pp. 1141-1148.

[19] P. Xu, J.Y. Zheng, P.F. Liu, Finite element analysis of burst pressure of composite hydrogen storage vessels, Mater. Des. 30, pp. 2295-2301, 2009.

[20] D.T.W. Lin, Y.C. Hu and C.H. Cheng, "The optimization of the thermal response on the ZnO flexible pyroelectric film temperature sensor," IEEE Sensors Journal, vol. 12, pp.397-403, 2012.

[21] D.T.W. Lin, C.N. Huang, and C.C. Chang, "The optimization of the heat removal on the LED package," Advanced Science Letters, vol. 4, pp. 2301-2305, 2011.

VI. BIOGRAPHIES

David T.W. Lin received the B.S. N.E. from National Tsing-Hua University, Tsinchu, Taiwan, in 1988, M.S.M.E. from Hua-Fan University, Taipei, Taiwan, in 1998, and PH.D. M.E. from Cheng Kung University, Tainan, Taiwan, in 2004, respectively. He is currently an associate professor at Graduate Institute of Mechatronic System Engineering, National University of Tainan. His main research interests are molecular dynamics, optimization, electronic device cooling, and inverse problem.

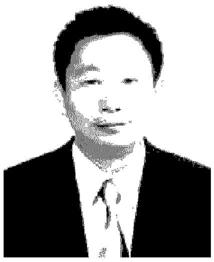

Figure Captions

Fig. 1 The mesh model of the 30° axisymmetric model with head of Al-carbon fiber/epoxy hydrogen pressure vessel.

Fig. 2 The flow chart of the optimal process.

Fig. 3 The initial stress distribution of the 30° axisymmetric model with head of Al-carbon fiber/epoxy hydrogen pressure vessel.

Fig. 4 The maximum stress profile with the SCGM iteration, the winding angle is [10˚ - 45˚], the thickness of composite layer is [1.2 - 1.6 mm.].

Fig. 5 The stress concentration with the winding angle from [10˚ - 45˚] at the thickness of composite layer is 1.6 mm.

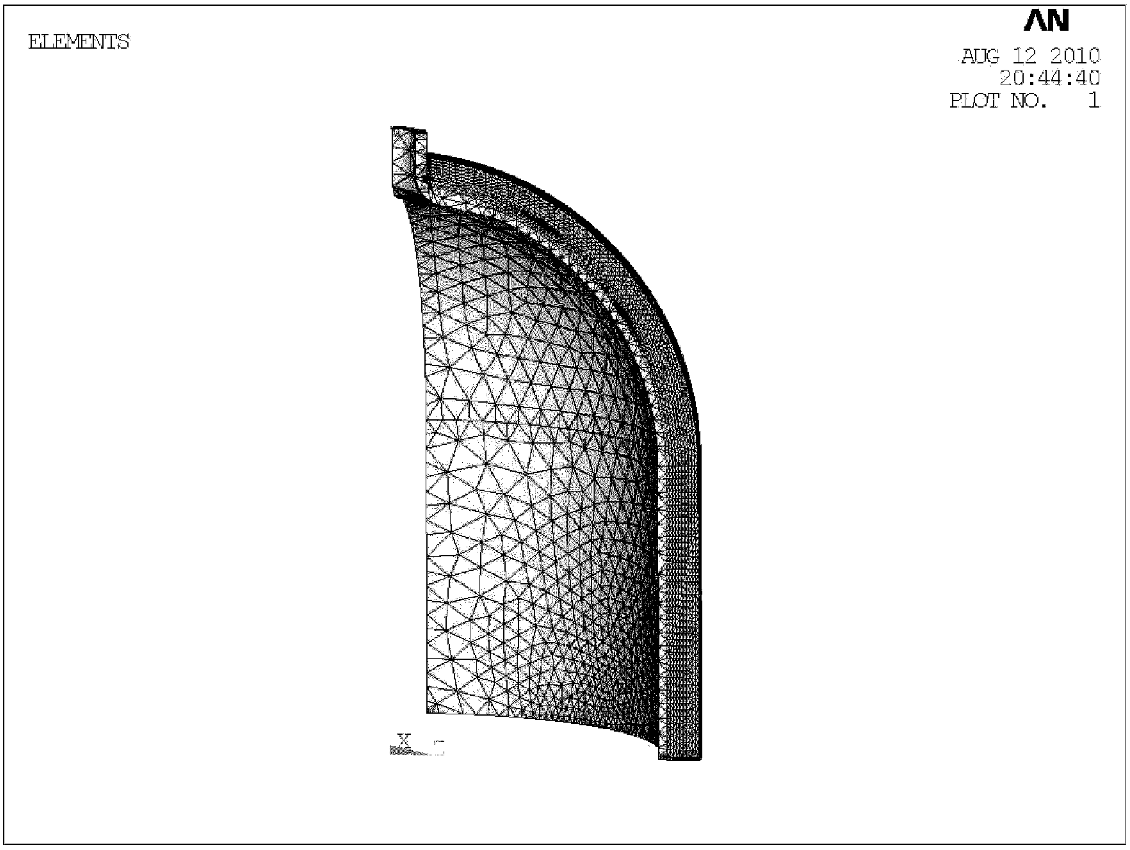

Fig. 1 The mesh model of the 30° axisymmetric model with head of Al-carbon fiber/epoxy hydrogen pressure vessel.

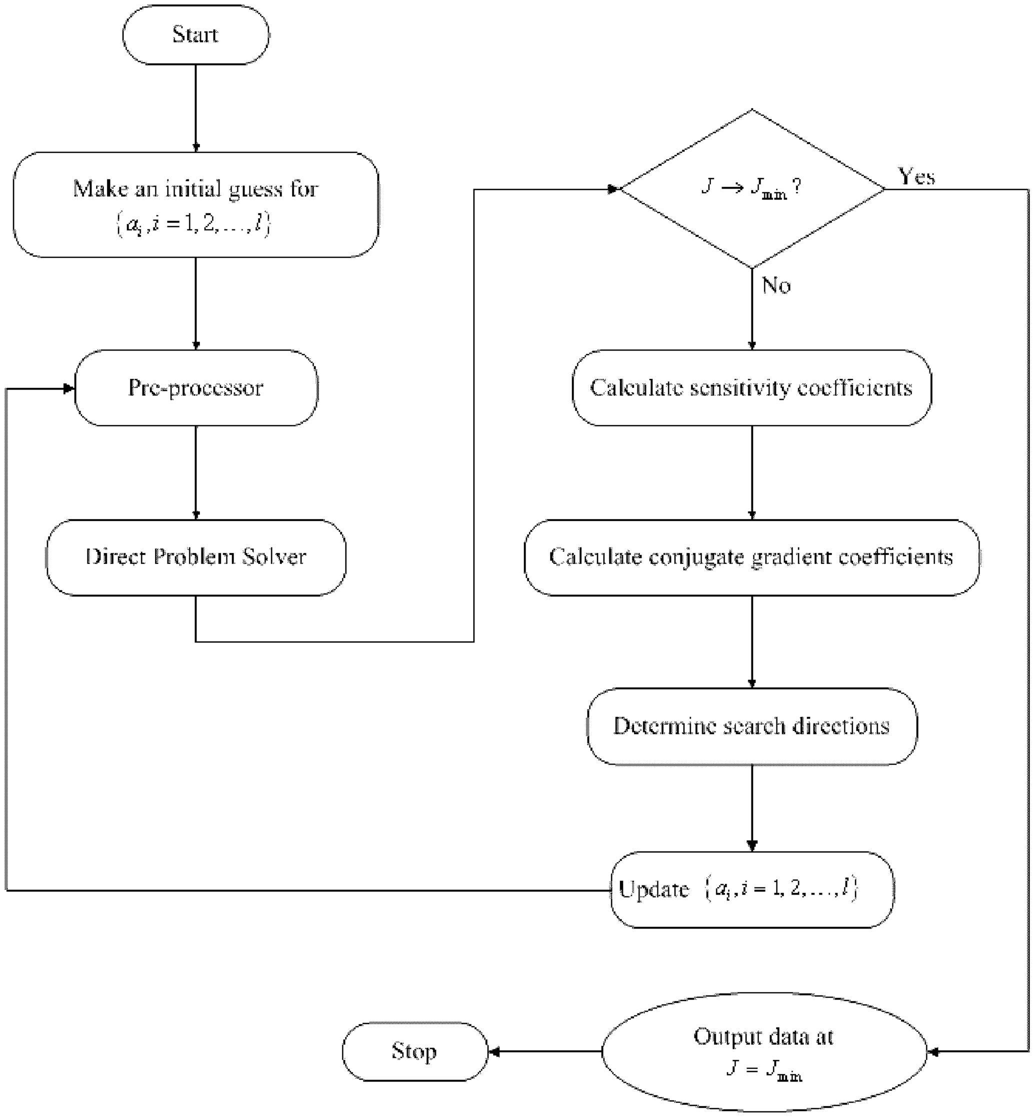

Fig.2 The flow chart of the optimal process.

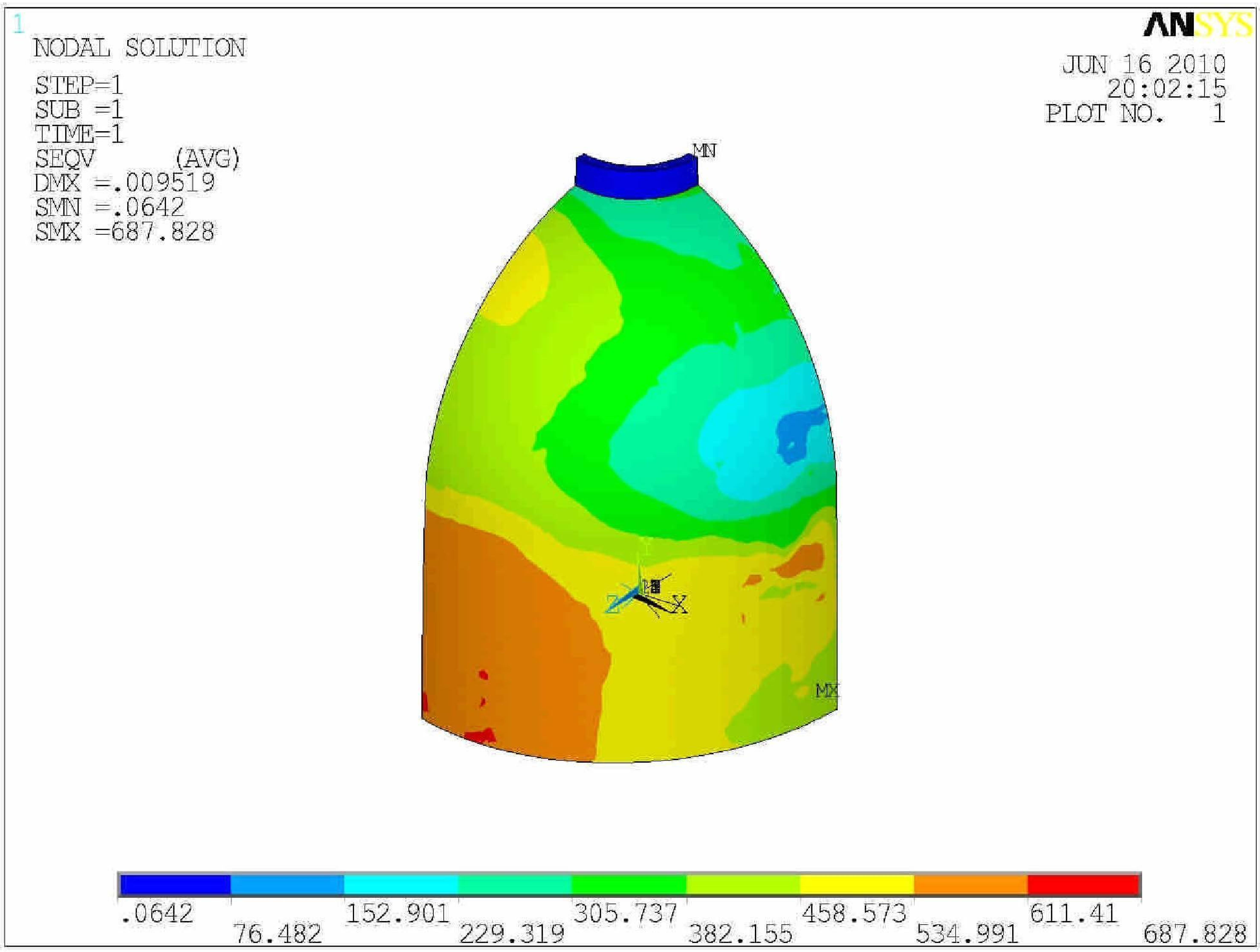

Fig. 3 The initial stress distribution of the 30° axisymmetric model with head of Al-carbon fiber/epoxy hydrogen pressure vessel.

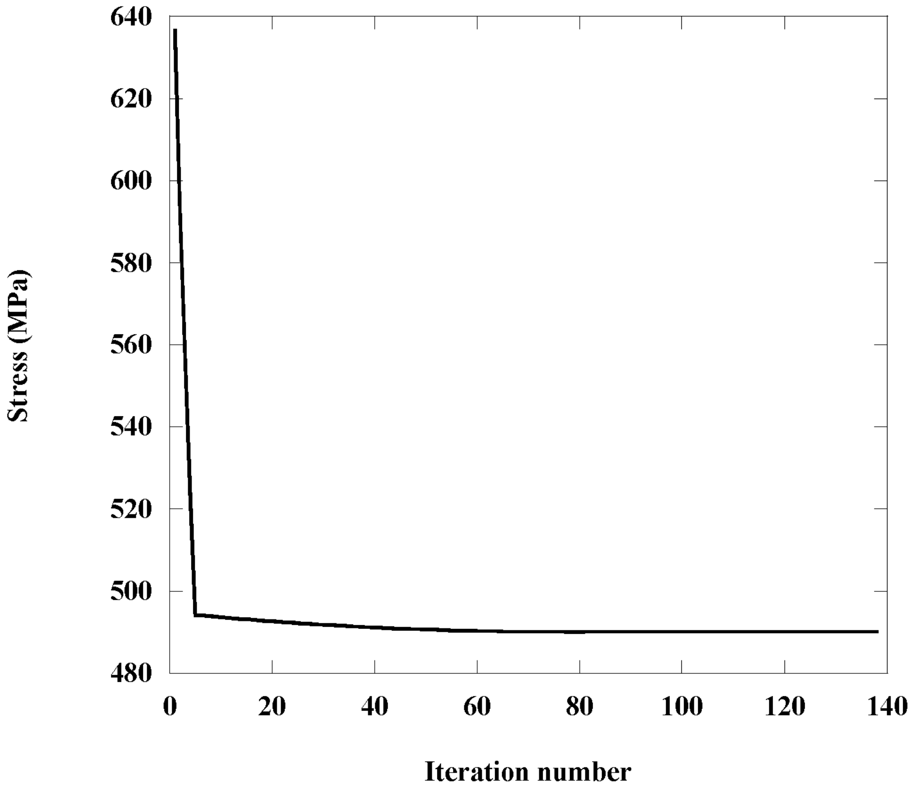

Fig. 4 The maximum stress profile with the SCGM iteration, the winding angle is [10° - 45°], the thickness of composite layer is [1.2 - 1.6 mm.].

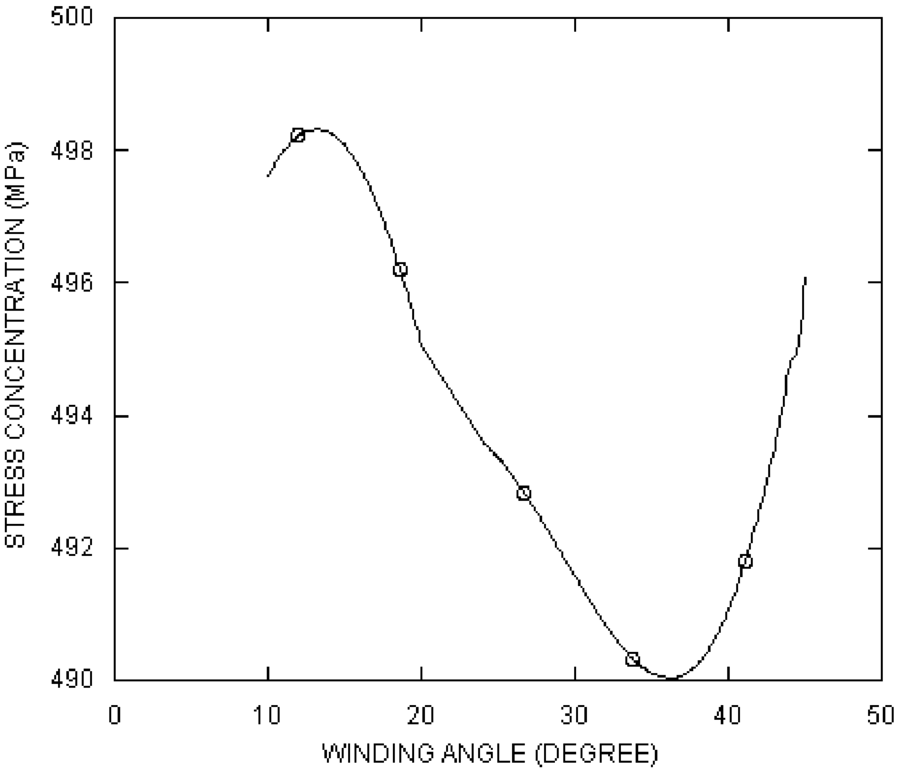

Fig. 5 The stress concentration with the winding angle from [10° - 45°] at the thickness of composite layer is 1.6 mm.